ISSN 1560-8034, 1605-6582 (On-line), SPQEO, 2019. V. 22, N 1. P. 26-33.

Semiconductor physics

Synthesis and characterization of new potassium-containing argyrodite-type compounds

I.P. Studenyak[1], A.I. Pogodin[1], V.I. Studenyak[1], O.P. Kokhan[1], Yu.M. Azhniuk[1,2], C. Cserháti[3], S. Kökényesi[3], D.R.T. Zahn[4]

[1]*Uzhhorod National University, Faculty of Physics*
3, Narodna Sq., 88000 Uzhhorod, Ukraine
[2]*Institute of Electron Physics, National Academy of Sciences of Ukraine, Uzhhorod, Ukraine*
[3]*Department of Experimental Physics, Faculty of Science and Technology, University of Debrecen,*
18/a Bem Sq., 4026 Debrecen, Hungary,
[4]*Semiconductor Physics, Chemnitz University of Technology,*
D-09107 Chemnitz, Germany
E-mail: studenyak@dr.com

Abstract. Potassium halogenthiophosphates K_6PS_5Br and K_6PS_5Cl as well as halogen-free K_7PS_6 compound were synthesized using the two-step technique from elemental substances as well as potassium halides. The elemental composition of the obtained samples was determined using energy-dispersive X-ray spectroscopy. Raman spectra of K_6PS_5Br and K_6PS_5Cl show themselves to be much similar to those of chemically related Cu_6PS_5Br and Cu_6PS_5Cl argyrodite crystals. The much richer spectra of K_6PS_5Br and K_6PS_5Cl as well as K_7PS_6, however, reveal that their structure most likely differs from the cubic structure of Cu_6PS_5Br and Cu_6PS_5Cl argyrodites.

doi: https://doi.org/10.15407/spqeo22.01.26
PACS 78.40.Ha; 77.80.Bh

Keywords: argyrodite, synthesis, scanning electron microscopy, Raman spectroscopy.

Manuscript received 28.12.18; revised version received 23.01.19; accepted for publication 20.02.19; published online 30.03.19.

1. Introduction

The family of argyrodite-structure compounds (the name originates from the argyrodite Ag_8GeS_6 mineral) includes a great number of representatives with a common chemical formula $A^{m+1}_{(12-n-x)/m}B^{n+}X^{2-}_{6-x}Y^{1-}$ $(0 < x < 1)$, where m and n are the valences of cations A = (Cu^+, Ag^+, Cd^{2+}, Hg^{2+}) and B = (Ga^{3+}, Si^{4+}, Ge^{4+}, P^{5+}, As^{5+}), respectively, with X = (S^{2-}, Se^{2-}, Te^{2-}) and Y = (Cl^-, Br^-, I^-) anions [1]. Some of them are known as superionic conductors promising for applications as solid electrolytes, supercapacitors, ion-selective membranes, and other electrochemical devices [2]. They are characterized by high electrical conductivity comparable to that of the best superionic conductors [3]. The most extensively studied are copper- and silver-containing argyrodites that were the subject of numerous studies (*e.g.* [4–8]). They are obtained in single-crystal, poly- and nanocrystalline forms, as composites, ceramics, and thin films [8–14]. For these materials, detailed structural, electrical, and optical studies were carried out, order/disorder processes and ion transport mechanisms were studied.

It was shown that structural disorder in the superionic phase of argyrodite crystals consists of two components – static and dynamic [8]. The former is related to the structure deficiency and leads to local non-uniform electric fields, which, in turn, result in additional smearing of band edges. Dynamic structural disorder appears in the superionic phase as hopping motion of mobile copper ions leading to high ionic conductivity. In the optical spectra, this disorder is revealed as the Urbach behaviour of the absorption edge in the superionic phase [5–8]. The electrical conductivity of copper-containing Cu_6PS_5I, Cu_6PS_5Br and Cu_6PS_5Cl argyrodites at 300 K and 1 kHz is 1.3×10^{-1} S/m, 1.2×10^{-3} S/m and 4.3 S/m, respectively [15].

For practical purposes, most suitable are argyrodite materials in the form of composites, ceramics, or thin films. For Cu_6PS_5I-based composites with polyvinyl-acetate, the electric conductivity is 7.2×10^{-2} S/m at 10^6 Hz [10], while for the composites of Cu_6PS_5I nanoparticles in a 6CB liquid crystal it increases to 4.8×10^{-6} S/m at 10^6 Hz [12]. For Cu_6PS_5I-based ceramics the total electrical conductivity increases with the grain size decrease: for the average grain size of 24 nm it

reaches 5.6×10^{-1} S/m at 10^6 Hz, a value typical for single-crystal Cu_6PS_5I [13]. Cu_6PS_5I-based thin films deposited by non-reactive radio-frequency magnetron sputtering are also characterized by the high electrical conductivity 5.2×10^{-2} S/m at 10^6 Hz [14].

In the recent decade, lithium-containing Li_6PS_5X (with X = Cl, Br and I) argyrodite superionic conductors have been actively studied as promising materials for all-solid-state batteries (ASSBs) [16–19]. It was demonstrated that ASSBs with oxygen-doped $Li_6PS_{5-x}O_xBr$ ($0 \le x \le 1$) superionic conductors can achieve higher capacities than oxygen-free superionic materials [20].

Even though the lithium-containing superionic conductors are very promising, the search for new superionic materials, in particular the sodium- or potassium-containing ones, is currently of great importance. This work is aimed at the synthesis and characterization of new potassium-containing argyrodite compounds which, to our knowledge, have not been reported so far.

2. Experimental

Potassium halogenthiophosphates K_6PS_5Cl and K_6PS_5Br were synthesized from high-purity elemental components: potassium 99.9 %, sulphur extra pure 15-3, phosphorus 99.9994% as well as chemically pure potassium chloride (bromide), additionally refined by directed crystallization from the melt. The two-temperature synthesis method was employed: stoichiometric amounts of the initial substances were loaded in a modified 140–160 mm long silica ampoule with the diameter 30…32 mm, which had an internal 80–100 mm long silica container with the diameter 18…20 mm. Potassium, phosphorus, and potassium chloride (bromide) were loaded in the internal container, while sulphur was loaded in the outer ampoule. The ampoules were pumped out to a residual pressure of 0.13 Pa and sealed before the synthesis.

The specially designed container with the loaded components was placed in a two-zone vertical resistive oven with electronically controlled temperatures. The apparatus design is shown in Fig. 1.

The synthesis of K_6PS_5Cl and K_6PS_5Br was performed by stepwise temperature increase with aging at 523 K for full fixation of sulphur and phosphorus. Under these conditions, potassium does not react with the container material, while the interaction with the sulphur vapour is slow, without intense heat liberation. Further heating was carried out at the rate 50 K/h up to the maximal temperature of 1100 K (K_6PS_5Cl) or 1060 K (K_6PS_5Br), which was by 50 K above the melting point for the binary compounds KCl and KBr, respectively. At this temperature, the melt was aged for 24 h with subsequent cooling down to 773…853 K (by 30 to 50 K above the crystallization point) with 24-h aging and further cooling down to the room temperature at a rate of 50 K/h. The synthesis resulted in visually polycrystal-like or glass-like materials of white or light yellow colour.

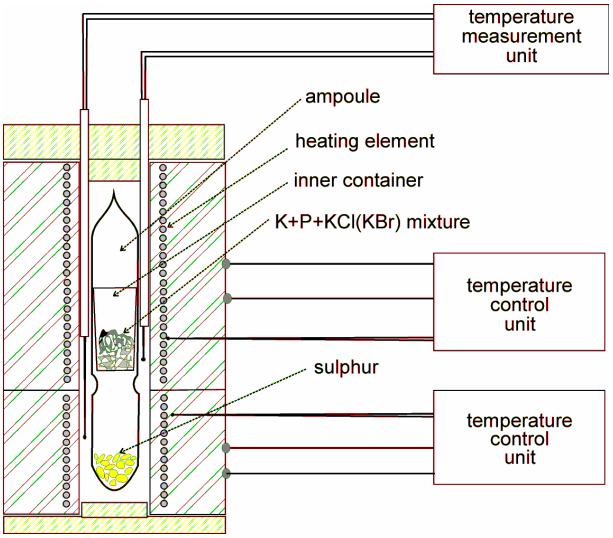

Fig. 1. Apparatus for potassium halogenthiophosphate synthesis.

The specimens obtained did not stick to the silica container or interact with its material.

Differential thermal analysis of the obtained samples was performed using combined chromel–alumel thermocouples at heating/cooling rates of 700 K/h. The accuracy of the temperature measurements was ±5 K.

Scanning electron microscopy (SEM) studies of the compounds were performed using the Hitachi S-4300 microscope. SEM studies were combined with energy-dispersive X-ray spectroscopy (EDX) to determine the chemical composition of the compounds.

Raman scattering measurements were carried out at room temperature using the Horiba LabRAM 800 spectrometer. Excitation was provided by a Cobolt Fandango solid-state laser with the excitation wavelength 514.7 nm. The signal was detected by a cooled CCD camera. The instrumental resolution was better than 2.5 cm^{-1}.

3. Results and discussion

The synthesized materials were studied by differential thermal analysis (see Fig. 2). The DTA curve for K_7PS_6 (Fig. 2a) does not exhibit noticeable anomalies in the heating or cooling curves. A slight endothermic effect of softening is observed in the heating curve at 607±5 K as well as a smeared exothermic effect of crystallization at 628±5 K, no exothermic effect of K_7PS_6 melting could be detected. Meanwhile, a slight exothermic effect of crystallization is observed at 687±5 K.

The K_6PS_5Cl DTA curve (Fig. 2b) is characterized by the presence of two endothermic effects at 735±5 K and 800±5 K in the heating curve and an exothermic effect in the cooling curve. The endothermic effect at 735±5 K is rather smeared, which can be an evidence for softening of a glassy phase within the range 735…782 K. Simultaneously, no clear exothermic effect of glass crystallization is observed. The endothermic effect at

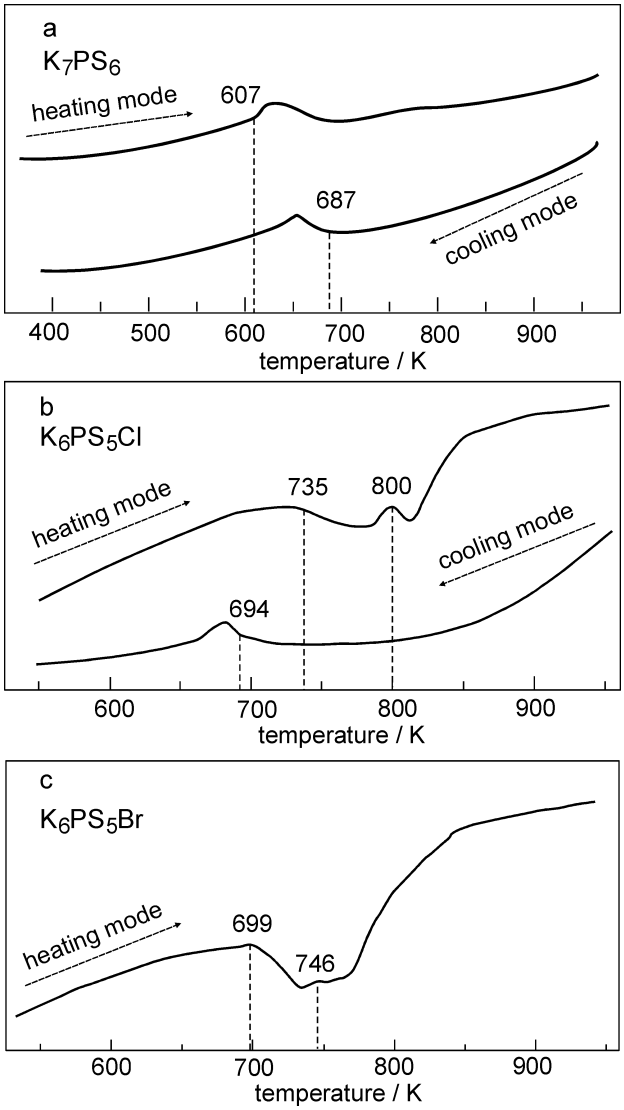

Fig. 2. DTA curves for the synthesized K_7PS_6, K_6PS_5Cl, and K_6PS_5Br samples.

800±5 K corresponds to K_6PS_5Cl melting. The cooling curve reveals a smeared exothermic effect of crystallization at the temperature 694±5 K. This difference between the temperatures of the corresponding effects in the heating and cooling curves can possibly be an evidence for a tendency to glass formation.

The DTA curve for K_6PS_5Br (Fig. 2c) exhibits two endothermic effects at 699±5 K and 746±5 K. Both effects are relatively slight and can be related to melting of a crystalline phase. Similarly to K_6PS_5Cl, the endothermic effect at 746±5 K corresponds to the K_6PS_5Br melting, while the first endothermic effect within the 699…735 K range is smeared and seems to be more typical for softening of a glassy phase.

SEM images of the synthesized potassium halogenthiophosphates shown in Fig. 3 reveal a visually polycrystal-like pattern with defined irregular domains of 20 to 200 μm size. The surface of the synthesized K_7PS_6 sample is much smoother (Fig. 4). EDX studies of the samples showed the chemical composition of the compounds to differ from the stoichiometry by no more than 10 % (*e.g.*, $K_{6.1\pm0.1}P_{1.1\pm0.1}S_{4.9\pm0.1}Cl_{0.9\pm0.1}$, $K_{7.2\pm0.1}P_{1.0\pm0.1}S_{5.8\pm0.1}$).

Raman spectra of the synthesized K_6PS_5Br and K_6PS_5Cl compounds are presented in Fig. 5. The spectra contain a set of quite narrow peaks, clearly revealing the crystalline character of the samples. The spectra show a noticeable similarity, with a dominating narrow (FWHM below 3 cm^{-1}) peak near 420 cm^{-1}. Comparison of the measured spectra with those of relatively well studied Cu_6PS_5Br and Cu_6PS_5Cl crystals with argyrodite structure [15, 21–23] grown by similar technique reveals similar features. Our experimentally measured Raman spectra of Cu_6PS_5Br and Cu_6PS_5Cl crystals were basically the same as those studied earlier [15]. For the copper-containing argyrodite crystals, the dominating peak near 420 cm^{-1} is assigned to symmetric vibrations of the PS_4 tetrahedra, which are the main structural units in the argyrodite lattice [15, 21-23]. The similar positions and intensities of this dominating narrow feature in the spectra make it reasonable to assume that the synthesized K_6PS_5Br and K_6PS_5Cl compounds are, similarly to Cu_6PS_5Br and Cu_6PS_5Cl, characterized by the argyrodite structure.

However, a more detailed look at the dominating peak (Fig. 6) shows that the spectra of K_6PS_5Br and

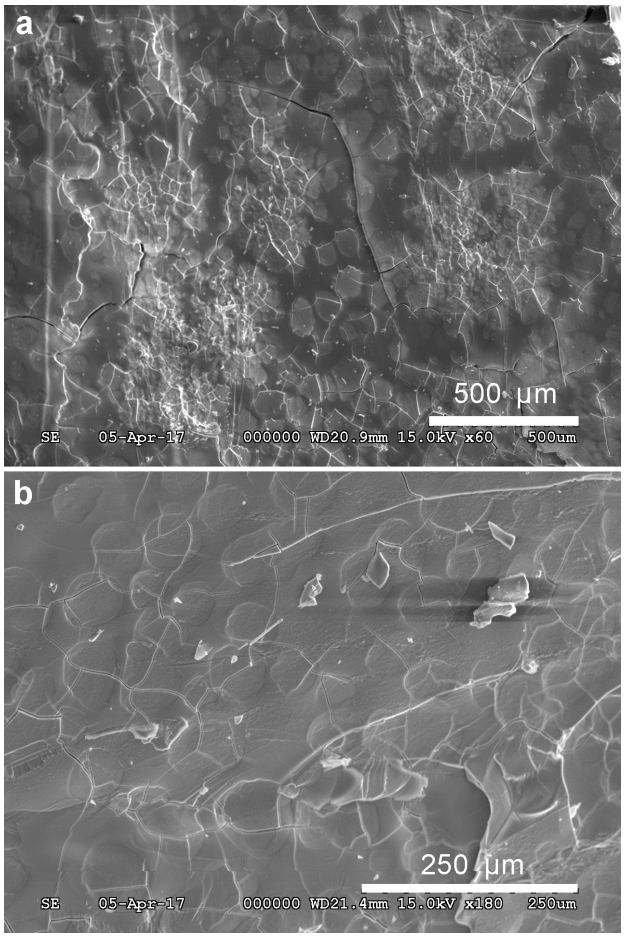

Fig. 3. SEM images of K_6PS_5Br (a) and K_6PS_5Cl (b) surfaces.

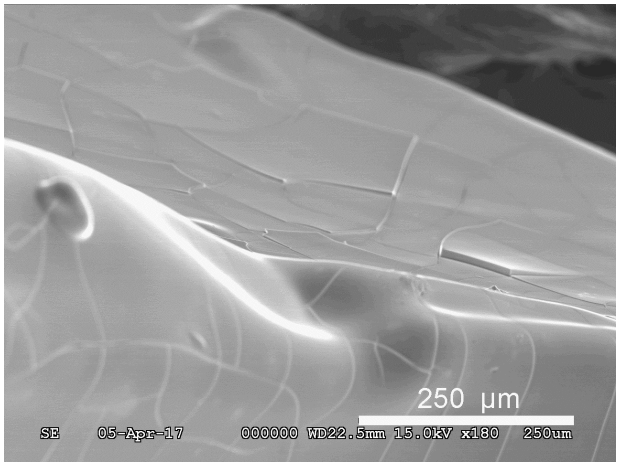

Fig. 4. SEM image of K_7PS_6 sample surface.

K_6PS_5Cl reveal distinct differences from those of the copper-containing argyrodites measured under the same experimental conditions. The most intense sharp peak in the spectra of Cu_6PS_5Br (418 cm^{-1}) and Cu_6PS_5Cl (421 cm^{-1}) is well described by a Lorentzian with FWHM of 9…11 cm^{-1}, which is very similar to the earlier data [15, 21, 23]. Meanwhile, the similar peak for K_6PS_5Br and K_6PS_5Cl is much narrower with a clearly visible shoulder at the lower-frequency side. Simulation of the observed feature by two Lorentzians reveals a superposition of two narrow peaks differing in frequency by 3 cm^{-1} (Fig. 6).

In general, the room-temperature Raman spectra of K_6PS_5Br and K_6PS_5Cl are much richer than those of the copper-containing counterparts. Namely, instead of a relatively weak and broad band near 540 cm^{-1}, which for Cu_6PS_5Br and Cu_6PS_5Cl is assigned to internal stretching vibrations of the PS_4 tetrahedra [15], for potassium halogenthiophosphates a series of narrow peaks within the range 530…575 cm^{-1} is observed. Note that for copper-containing argyrodites splitting of the broad band into several features is revealed at low temperatures [15].

In the lower-frequency range (below 400 cm^{-1}), there is no visible correlation between the room-temperature Raman spectra of copper and potassium halogenthiophosphates. The spectra of K_6PS_5Br and K_6PS_5Cl contain much more peaks that are considerably narrower than those of the copper-containing counterparts. A doublet observed for potassium-containing argyrodites within the range 267…274 cm^{-1} is most likely related to bending vibrations of the PS_4 tetrahedral groups. Their counterparts in Cu_6PS_5Br and Cu_6PS_5Cl spectra are relatively broad features near 310 cm^{-1} corresponding to doubly and triply degenerate E and F_2 bands which are known to be resolved at lower temperatures [15]. A somewhat broader (16–18 cm^{-1}) feature near 210 cm^{-1} in the spectra of K_6PS_5Br and K_6PS_5Cl does not have a direct counterpart in the room-temperature Raman spectra of Cu_6PS_5Br and Cu_6PS_5Cl, but most likely corresponds to the vibrations reported for copper-containing argyrodites at 77 K within the range 220…230 cm^{-1}. Weak features observed at 85 and 98 cm^{-1} (for both K_6PS_5Br and K_6PS_5Cl) as well as 124 and 143 cm^{-1} (for K_6PS_5Cl only) can be assigned to external translational and librational vibrations with the participation of sulphur, potassium, and halogen atoms.

Two groups of Raman features reveal the most noticeable difference between the potassium-containing and copper-containing halogenthiophosphates as well as between K_6PS_5Br and K_6PS_5Cl. While for Cu_6PS_5Br and Cu_6PS_5Cl no features are observed in the high-frequency region between the most intense peak near 420 cm^{-1} and the low-intensity maximum near 540 cm^{-1} even at low temperatures, for K_6PS_5Br one can clearly observe a maximum at 465 cm^{-1} while for K_6PS_5Cl an intense rather sharp doublet is revealed at 446 and 451 cm^{-1} as well as a weaker shoulder at 463 cm^{-1}. At somewhat lower frequencies, a weak band is observed at 361 cm^{-1} for K_6PS_5Br and a roughly equally weak triplet within the range 336…346 cm^{-1} is registered for K_6PS_5Cl, with no counterparts in the spectra of the copper-containing argyrodites.

In spite of the observed differences, one can assume, based on the general similarity of the Raman spectra of the synthesized K_6PS_5Br and K_6PS_5Cl and the known Cu_6PS_5Br and Cu_6PS_5Cl crystals, that all these materials belong to the argyrodite family with pronounced PS_4 tetrahedral structural groups. Still,

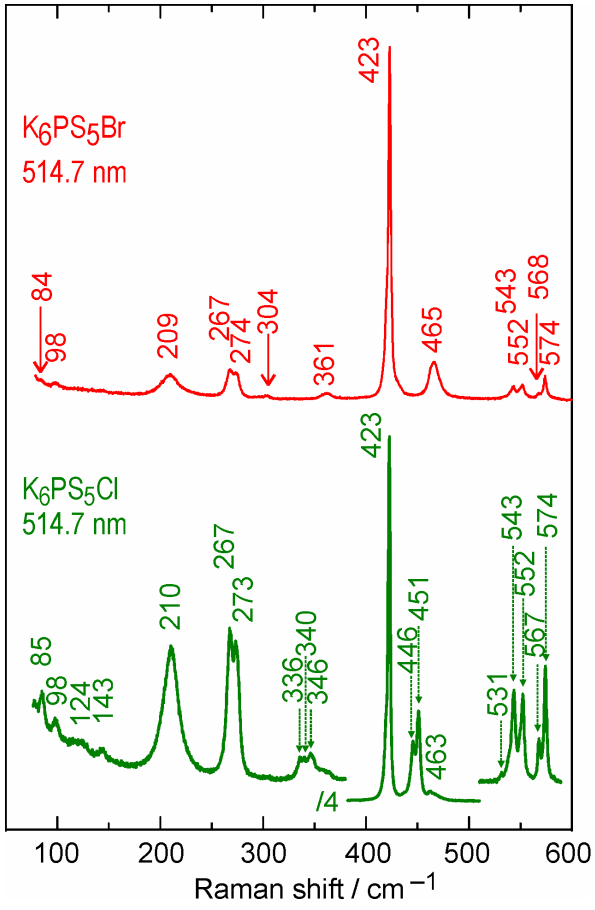

Fig. 5. Raman spectra of K_6PS_5Br and K_6PS_5Cl crystals.

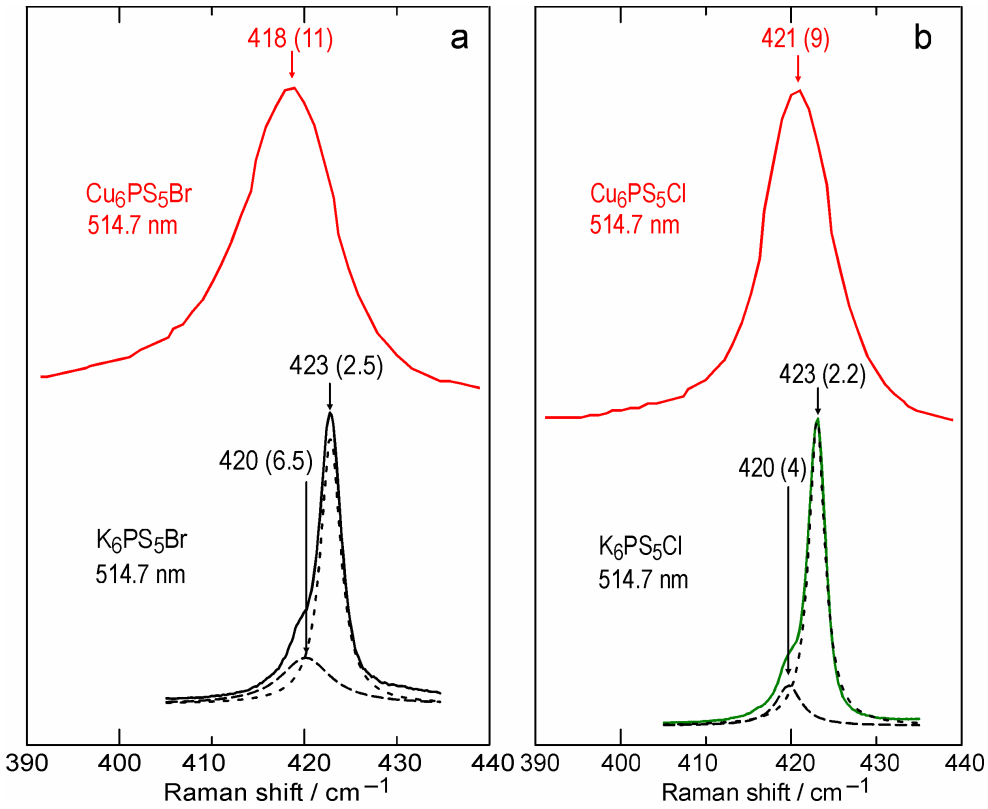

Fig. 6. Zoomed view of the dominating feature in the Raman spectra of Cu_6PS_5Br and K_6PS_5Br (a) as well as Cu_6PS_5Cl and K_6PS_5Cl (b) crystals. The observed peak is approximated by one (where appropriate) or two Lorentzians. The frequencies and halfwidths (in parentheses) of the fitting contours are indicated.

there are some rather systematic differences in the Raman spectra of K_6PS_5Br and K_6PS_5Cl, on the one hand, and Cu_6PS_5Br and Cu_6PS_5Cl, on the other hand which can be explained by several factors. First of all, the broader spectral features of copper-containing argyrodite crystals in comparison with those of K_6PS_5Br and K_6PS_5Cl can be related to the lower rigidity of the Cu_6PS_5Br and Cu_6PS_5Cl crystal lattice since these materials are known to possess high ionic conductivity at room temperature [1, 9]. Even though the ionic conductivity is related to mobile copper ions, the vibrations of which have lower frequencies and are external with respect to the pronounced PS_4 tetrahedral structural groups, the ionic motion evidently contributes to the increase of the damping of their vibrations revealed as somewhat broader peaks in the Cu_6PS_5Br and Cu_6PS_5Cl Raman spectra. The high ionic mobility in copper-containing argyrodites can also be responsible for the fact that broad maxima in the room-temperature Raman spectra of these compounds can be split into narrower features only at lower temperatures [15].

The appearance of multiple narrow peaks in the higher-frequency range of the K_6PS_5Br and K_6PS_5Cl Raman spectra (four distinct features within the 530…575 cm^{-1} range, the intense new peaks within the 445…465 cm^{-1} range, and the clearly resolved doublet structure of the most intense peak), as compared to those of the copper-containing argyrodites, can be evidence for a difference in the crystal structure of potassium-containing compounds. It is well known that crystals of the argyrodite family can possess not only cubic (like Cu_6PS_5Br and Cu_6PS_5Cl), but also hexagonal [24], orthorhombic [25], or monoclinic [26] structure. A non-cubic argyrodite structure of potassium halogen-thiophosphates could be a possible reason for splitting of the modes at 267 and 273 cm^{-1}, which correlate with degenerate vibrations of E and F_2 symmetry near 310 cm^{-1} in Cu_6PS_5Br and Cu_6PS_5Cl.

Alternatively, the numerous distinct features in the Raman spectra of the synthesized K_6PS_5Br and K_6PS_5Cl compounds can possibly be related to the presence of different crystalline polythiophosphate species, the structure of which can contain tetrahedra of similar type, with or without distortion, providing the corresponding different vibration frequencies being revealed. It is known from our recent studies [22, 23] that, for instance, Cu_7PS_6, although possessing a different symmetry group, has a very similar most prominent Raman feature at 425 cm^{-1}, corresponding to symmetric vibrations of the PS_4 tetrahedra. From this point of view, it seemed interesting to compare these data with those of Raman measurements performed for the synthesized halogen-free K_7PS_6 compound. From the corresponding spectra, shown in Fig. 7, one can clearly see that the similarity between K_7PS_6 and Cu_7PS_6 is much smaller than the similarity between K_7PS_6 and the potassium-containing halogenthiophosphates. In particular, one can clearly notice the agreement of the peak frequencies at 445 and

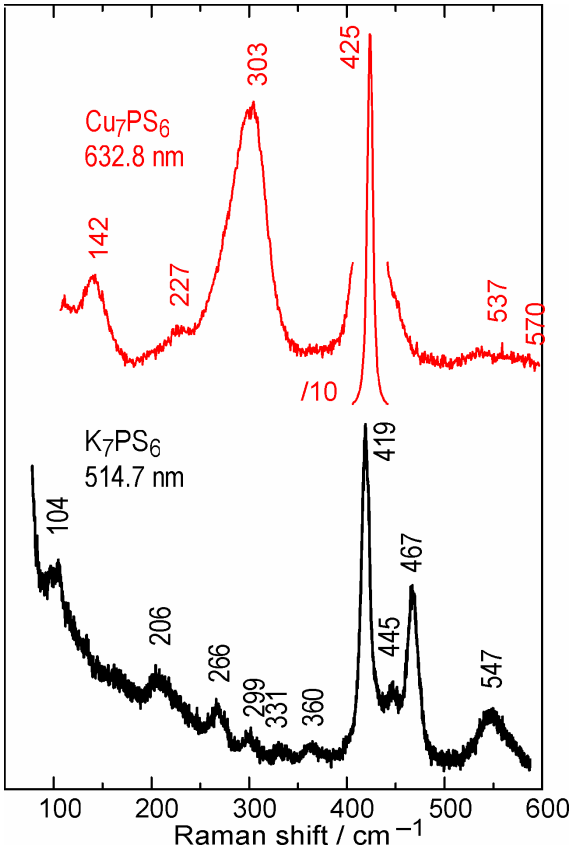

Fig. 7. Comparison of the Raman spectra of K_7PS_6 and Cu_7PS_6 compounds.

467 cm^{-1} in the spectrum of K_7PS_6 (Fig. 7) with those observed for K_6PS_5Br and K_6PS_5Cl (Fig. 5). On the one hand, as noted above, this could possibly mean that the synthesized potassium halogenthiophosphate compounds may have some K_7PS_6 crystallites that thus leave their fingerprints in the Raman spectra. However, it seems much more realistic that the structure of the argyrodite compounds under investigation depends on the cation species much stronger as it could be initially expected.

4. Conclusions

Potassium halogenthiophosphates K_6PS_5Br and K_6PS_5Cl as well as halogen-free K_7PS_6 compound, which, to our knowledge, have not been reported before, were synthesized by a two-step technique from elemental substances as well as potassium halides. The elemental composition of the samples was determined by EDX. Raman spectra of K_6PS_5Br and K_6PS_5Cl samples provide evidence for their crystalline structure. Their comparison with the Raman spectra of chemically related Cu_6PS_5Br and Cu_6PS_5Cl argyrodites confirmed that K_6PS_5Br and K_6PS_5Cl also belong to the argyrodite family. However, the much richer spectrum of K_6PS_5Br and K_6PS_5Cl as well as K_7PS_6 in comparison with the copper-containing related compounds implies that the structure of potassium-containing argyrodites most likely differs from the cubic structure of Cu_6PS_5Br and Cu_6PS_5Cl argyrodites.

Acknowledgement

Yu.M. Azhniuk is grateful to DFG Research Unit FOR 1154 “Towards Molecular Spintronics” for the financial support of his research at Chemnitz University of Technology.

References

1. Kuhs W.F., Nitsche R., Scheunemann K. The argyrodites – a new family of the tetrahedrally close-packed structures. *Mat. Res. Bull.* 1979. **14**. P. 241–248.
2. Nilges T., Pfitzner A. A structural differentiation of quaternary copper argyrodites: Structure – property relations of high temperature ion conductors. *Z. Kristallogr.* 2005. **220**. P. 281–294.
3. Studenyak I.P., Kranjčec M., Bilanchuk V.V., Kokhan O.P., Orliukas A.F., Kazakevicius E., Kezionis A., Salkus T. Temperature variation of electrical conductivity and absorption edge in Cu_7GeSe_5I advanced superionic conductor. *J. Phys. Chem. Solids.* 2009. **70**. P. 1478–1481.
4. Laqibi M., Cros B., Peytavin S., Ribes M. New silver superionic conductors Ag_7XY_5Z (X = Si, Ge, Sn; Y = S, Se; Z = Cl, Br, I) – synthesis and electrical studies. *Solid State Ionics*. 1987. **23**. P. 21–26.
5. Studenyak I.P., Kranjčec M., Kovacs Gy.S., Desnica-Franković I.D., Panko V.V., Guranich P.P. Electric conductivity and optical absorption edge of $Cu_6P(Se_xS_{1-x})_5I$ fast-ion conductors in the selenium-rich region. *J. Phys. Chem. Solids*. 2001. **62**. P. 665–672.
6. Studenyak I.P., Kranjčec M., Kovacs Gy.S., Desnica-Franković I.D. et al. The excitonic processes and Urbach rule in $Cu_6P(S_{1-x}Se_x)_5I$ crystals in the sulfur-rich region. *Mat. Res. Bull.* 2001. **36**. P. 123–135.
7. Kranjčec M., Studenyak I.P., Bilanchuk V.V., Dyordyaj V.S., Panko V.V. Compositional behaviour of Urbach absorption edge and exciton-phonon interaction parameters in $Cu_6PS_5I_{1-x}Br_x$ superionic mixed crystals. *J. Phys. Chem. Solids.* 2004. **65**. P. 1015–1020.
8. Kranjčec M., Studenyak I.P., Kurik M. Urbach rule and disordering processes in $Cu_6P(S_{1-x}Se_x)_5Br_{1-y}I_y$ superionic conductors. *J. Phys. Chem. Solids*. 2006. **67**. P. 807–817.
9. Beeken R.B., Garbe J.J., Petersen N.R. Cation mobility in the Cu_6PS_5X (X = Cl, Br, I) argyrodites. *J. Phys. Chem. Solids*. 2003. **64**. P. 1261–1264.
10. Orliukas A.F., Kazakevicius E., Kezionis A. et al. Preparation, electric conductivity and dielectrical properties of Cu_6PS_5I-based superionic composites. *Solid State Ionics*. 2009. **180**. P. 183–186.
11. Salkus T., Galeckas V., Badot J.C., Studenyak I.P., Makauz I.I., Selskis A., Kezionis A., Banys J. Impedance spectroscopy study of Cu_6PS_5I-As_2S_3 nanocomposites. *Ionics.* 2013. **19**. P. 1387–1391.

12. Studenyak I.P., Izai V.Yu., Studenyak V.I., Kovalchuk O.V., Kovalchuk T.M., Kopčanský P., Timko M., Tomašovičová N., Zavisova V., Miskuf J., Oleinikova I.V. Influence of Cu_6PS_5I superionic nanoparticles on the dielectric properties of 6CB liquid crystal. *Liquid Crystals*. 2017. **44**. P. 897–903.
13. Šalkus T., Kazakevičius E., Banys J., Kranjčec M., Chomolyak A.A., Neimet Yu.Yu., Studenyak I.P. Influence of grain size effect on electrical properties of Cu_6PS_5I superionic ceramics. *Solid State Ionics*. 2014. **262**. P. 597–600.
14. Studenyak I.P., Kranjčec M., Izai V.Yu., Chomolyak A.A., Vorohta M., Matolin V., Cserhati C., Kökényesi S. Structural and temperature-related disordering studies of Cu_6PS_5I amorphous thin films. *Thin Solid Films*. 2012. **520**. P. 1729–1733.
15. Studenyak I.P., Stefanovich V.O., Kranjčec M., Desnica I.D., Azhnyuk Yu.M., Kovacs Gy.Sh., Panko V.V. Raman scattering studies of Cu_6PS_5Hal (Hal = Cl, Br, I) fast-ion conductors. *Solid State Ionics.* 1997. **95**. P. 221–225.
16. Yu C., van Eijck L., Ganapathy S., Wagemaker M. Synthesis, structure and electrochemical performance of the argyrodite Li_6PS_5Cl solid electrolyte for Li-ion solid state batteries. *Electrochimica Acta*. 2016. **215**. P. 93–99.
17. Auvergniot J., Cassel A., Foix D., Viallet V., Seznec V., Dedryvère R. Redox activity of argyrodite Li_6PS_5Cl electrolyte in all-solid-state Li-ion battery: An XPS study. *Solid State Ionics.* 2017. **300**. P. 78–85.
18. Wenzel S., Seldmaier S.J., Dietrich C., Zeier W.G., Janek J. Interfacial reactivity and interphase growth of argyrodite solid electrolytes at lithium metal electrodes. *Solid State Ionics.* 2018. **318**. P. 102–112.
19. Yubuchi S., Uematsu M., Hotehama C., Sakuda A., Hayashi A., Tatsumisago M. An argyrodite sulfide-based superionic conductor synthesized by a liquid-phase technique with tetrahydrofuran and ethanol. *J. Mater. Chem.* 2019. **A** 7. P. 558–566.
20. Zhang Z., Zhang L., Yan X., Wang H., Liu Y., Yu C., Cao X., van Eijck L., Wen B. All-in-one improvement toward Li_6PS_5Br-based solid electrolytes triggered by compositional tune. *J. Power Sources*. 2019. **410–411**. P. 162–170.
21. Kranjčec M., Studenyak I.P., Buchuk R.Yu., Stephanovich V.O., Kökényesi S., Kis-Varga M. Structural properties and Raman scattering in Cu_6PS_5X (X = I, Br) nanocrystalline solid electrolytes. *Solid State Ionics*. 2008. **179**. P. 218–221.
22. Studenyak I.P., Luchynets M.M., Izai V.Yu., Pogodin A.I., Kokhan O.P., Azhniuk Yu.M., Zahn D.R.T. Structure and Raman spectra of $(Cu_6PS_5I)_{1-x}(Cu_7PS_6)_x$ mixed crystals. *Semiconductor Physics, Quantum Electronics & Optoelectronics*. 2017. **20**. P. 369–374.
23. Studenyak I.P., Luchynets M.M., Izai V.Yu., Pogodin A.I., Kokhan O.P., Azhniuk Yu.M., Zahn D.R.T. Structural properties, Raman spectra, and diffuse reflectivity of $(Cu_6PS_5Br)_{1-x}(Cu_7PS_6)_x$ mixed crystals. *J. Alloys and Compounds*. 2019. **782**. P. 586–591.
24. Jaulmes S., Julien-Pouzol M., Laruelle P., Rivet J. Varietes de haute et basse température du séléniure double de cuivre et de germanium. *Acta Crystallographica*. 1991. **C47**. (1799–1803.
25. Eulenberger G. Die Kristallstruktur der Tieftemperaturmodifikation von Ag_8GeS_6. *Monatshefte für Chemie*. 1977. **108**. P. 901–913.
26. Haznar A., Pietraszko A., Studenyak I.P. X-ray study of the superionic phase transition in Cu_6PS_5Br. *Solid State Ionics.* 1999. **119**. P. 31–36.

Authors and CV

Ihor P. Studenyak, born in 1960, defended his Dr. Sc. degree in Physics and Mathematics in 2003 and became full professor in 2004. Vice-rector for research at Uzhhorod National University, Ukraine. Authored over 200 publications, 120 patents, 15 textbooks. The area of his scientific interests includes physical properties of semiconductors, ferroics and superionic conductors.

Artem I. Pogodin, born in 1988, defended his PhD thesis in inorganic chemistry in 2016. Senior researcher at Uzhhorod National University. Authored over 35 articles and 25 patents. The area of his scientific interests includes solid state chemistry, crystal growth, and materials science.

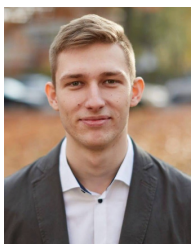

Viktor I. Studenyak, born in 1997. At present he is a master student at Faculty of Physics, Uzhhorod National University. Authored 7 articles and 5 patents. The area of his scientific interests includes optical properties of superionic conductors.

Oleksandr P. Kokhan, born in 1958, defended his PhD thesis in inorganic chemistry in 1996 and became docent in 2002. Associate professor of Inorganic Chemistry department at Uzhhorod National University. Authored over 80 articles and 40 patents. The area of his scientific interests includes inorganic chemistry, solid state chemistry, crystal growth, materials science.

Yuriy M. Azhniuk, born in 1961, accomplished his Dr. Sc. (equiv. to Hab. Dr.) degree in Semiconductor Physics in 2011. Senior Researcher at Institute of Electron Physics, NAS of Ukraine and Uzhhorod National University, Ukraine. Authored over 80 papers. The area of his scientific interests includes semiconductor physics, nanophysics, and Raman spectroscopy.

Csaba Cserháti, born in 1963, defended his PhD degree in Physics in 1995. He is an associate professor in University of Debrecen, Hungary. Authored over 100 publications. The area of his scientific interests is materials science.

Sandor Kökényesi, born in 1946, defended his PhD Dissertation in Physics and Mathematics in 1973, became DSc in 1990 and full professor in 1991. Head of Department at Uzhhorod National University till 2000, later up to now Scientific Advisor, Emeritus at the University of Debrecen, Hungary. Authored over 200 scientific publications, 20 patents. The area of scientific interests relates materials science, photonics, nanotechnology.

Dietrich R.T. Zahn, accomplished his Ph. D. degree in 1988 at University of Wales, Cardiff, UK. Professor of Semiconductor Physics at Chemnitz University of Technology, Chemnitz, Germany since 1993. Council Member of the German Physical Society (DPG), Member of the EPSRC Peer Review College, Vice-President of the German Vacuum Society (DVG). Authored over 650 papers in peer-reviewed journals. The area of his scientific expertise includes semiconductor physics, nanophysics, physics of surfaces and interfaces.